Non-Hermitian dispersion sign reversal of radiative resonances in two dimensions

R. Binder,[1,2,*] J. R. Schaibley,[2] and N. H. Kwong[1]
[1]*Wyant College of Optical Sciences, The University of Arizona, Tucson, Arizona 85721, USA*
[2]*Department of Physics, The University of Arizona, Tucson, Arizona 85721, USA*

(Received 7 August 2023; revised 9 February 2024; accepted 13 February 2024; published 1 March 2024)

In a recent publication [Wurdack *et al.*, Nat. Commun. **14**, 1026 (2023)], it was shown that in microcavities containing atomically thin semiconductors, non-Hermitian quantum mechanics can lead to negative exciton polariton masses. Here, we study the mass-sign reversal in two-dimensional systems and show that it is not contingent on the cavity. We show that it can occur generally in radiative resonances in two dimensions and derive conditions for it (critical dephasing threshold, etc.). In monolayer transition-metal dichalcogenides, this phenomenon is not invalidated by the strong electron-hole exchange interaction, which is known to make the exciton massless.

DOI: 10.1103/PhysRevB.109.125301

I. INTRODUCTION

Non-Hermitian quantum mechanics has recently attracted much interest, both in terms of general physics (a recent review article is Ref. [1], a recent textbook Ref. [2]) and also in the area of optics (review article Ref. [3]). While the concept of exceptional points [4–6] is certainly one major driving force behind this increasing interest (see for example Refs. [7–20]), it is only now emerging that non-Hermtian quantum mechanics can lead to other novel phenomena that are not expected on the basis of Hermitian physics. For example, in Ref. [21] it was shown that in a microcavity containing a transition-metal dichalcogenides (TMD) monolayer, non-Hermitian quantum mechanics can drastically change the exciton dispersion [22–25] and lead to negative exciton polariton masses. Mass renormalization is a standard concept in many-particle physics; for example, the coupling of electrons to the lattice vibrations leads to quasiparticles called polarons, whose effective mass differs from that of the electrons (p. 496 of [26]). In semiconductor quantum well microcavities, coupling of an exciton resonance to the light field yields the polariton whose effective mass is usually much smaller than that of the exciton (e.g., [27]). But non-Hermitian effects are usually associated with simple line broadenings or lifetime reductions, not with qualitative effects such as strong mass renormalization or even reversal of the sign of the effective mass.

Radiative resonances (such as excitons) in two-dimensional (2D) layers emit light into the surrounding 3D space. In cavities, this light is reflected back to the layer, similar to an optical feedback, which then transforms the excitons into cavity polaritons. The phenomenon of mass-sign reversal was demonstrated in Ref. [21] for such polaritons in semiconductor microcavities. The question then arises whether the optical feedback from the cavity is needed for the mass-sign reversal to occur, or whether more generally the mass-sign reversal can occur in two-dimensional systems without the optical feedback from the cavity. We show here that the latter is the case: that mass-sign reversal is possible in any 2D system with a massive resonance coupled to the radiation field (if the mass of the resonance is infinite before the coupling, a finite negative mass can be generated). We call the electromagnetic modes coupled to the material polarization "2D-layer polaritons" (in the literature they are also sometimes referred to as "quantum well polaritons"). We derive an analytic expression for the critical dephasing [28] at which the mass diverges and changes sign, and we discuss an analytical condition for such a sign reversal to be possible (which we find to be strongly affected by the dielectric environment). While the effective mass is related to the second-order Taylor expansion of the dispersion with respect to the wave vector, we find that for nonzero dephasings that are much smaller than the critical dephasing, a sign reversal of the dispersion of orders higher than two leads to an energy minimum on a ring at the edge of the radiative cone. Similar to the predictions for microcavities [21], the effective mass reversal will affect possible Bose Einstein condensates (BECs). In the present case of single layers or quantum wells, we speculate this would either lead to conical emission or directional symmetry breaking of the emission (i.e., the BEC would have one more broken-symmetry variable in addition to the phase of the condensate wave function). We also clarify that the sign reversal is not affected by the long-range electron-hole exchange interaction [22,23,25,29–32], which is known to be strong in monolayer TMDs and to give approximately linear (i.e., massless) exciton dispersions.

II. THEORY OF 2D-LAYER POLARITONS

We assume the 2D system (e.g., TMD monolayer or thin quantum well) to be in the x-y plane at $z = z_0 = 0$ and to have a discrete optical resonance described by the polarization $\mathbf{P}^{3D} = \delta(z - z_0)\mathbf{P}(\mathbf{q}, \omega)$, where $\mathbf{P}(\mathbf{q}, \omega)$ is the 2D polarization. We assume the layer to be sufficiently thin so that the z dependence of $\mathbf{P}^{3D}$ can be approximated by the δ function.

*Corresponding author: binder@optics.arizona.edu

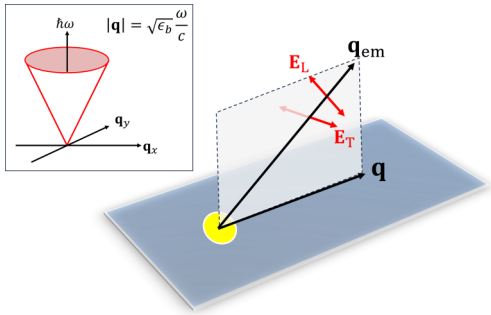

FIG. 1. Sketch of 2D-layer exciton polariton with exciton (yellow dot) propagating with wave vector $\mathbf{q}$ in the plane of the layer, and emitted p-polarized (s-polarized) radiation field $\mathbf{E}_L$ ($\mathbf{E}_T$) with wave vector $\mathbf{q}_{em}$. Inset: radiative cone.

The geometry is schematically shown in Fig. 1. Maxwell's propagation equation for the in-plane components of the light field (electric field) amplitude, $E_j(\mathbf{q}, z, \omega)$, then reads

$$\left\{-q^2 + \frac{\partial^2}{\partial z^2} + \epsilon_b \frac{\omega^2}{c^2}\right\} E_j(\mathbf{q}, z, \omega) = -\delta(z - z_0)\eta_v \left[\frac{4\pi\omega^2}{c^2} P_j(\mathbf{q}, \omega) - \frac{4\pi}{\epsilon_b} q_j \mathbf{q} \cdot \mathbf{P}(\mathbf{q}, \omega)\right]. \tag{1a}$$

Here, $j = x, y$ labels the Cartesian component, $q = \sqrt{q_x^2 + q_y^2}$ is the magnitude of the in-plane wave vector, ϵ_b the background dielectric constant, and η_v the multiplicity of equivalent valleys ($\eta_v = 3$ in TMDs, $\eta_v = 1$ in GaAs). The last term in the square bracket stems from the $\nabla(\nabla \cdot \mathbf{E})$ term in the propagation equation, which in turn comes from the $\nabla \times (\nabla \times \mathbf{E})$ term. In the following, we assume $\mathbf{q} = (q_x, 0)$, so that E_x is the longitudinal (L) and E_y the transverse (T) field component. While the following discussion is valid for any physical realization of the optical resonance, we use terminology appropriate for our example, which is the $1s$ exciton in a direct-gap semiconductor such as a GaAs quantum well [33–38] or semiconducting TMD monolayer [22,23,39–58]. The polarization components $P_{x,y}(\mathbf{q}, \omega) = \eta_v D_0^* p^{1s}_{x,y}(\mathbf{q}, \omega)$ are then a product of the interband dipole matrix element $D_0 = e r_{cv} \phi_{1s}(r = 0)$, where $\phi_{1s}(r = 0)$ is the $1s$ exciton wavefunction at zero relative coordinate, e is the electron charge and er_{cv} the interband dipole matrix element (for a detailed discussion see Ref. [59]), and the interband coherence of the $1s$ exciton $p^{1s}_{x,y}$, which in linear optical response obeys the equation of motion

$$i\hbar \frac{\partial}{\partial t} p_j^{1s}(\mathbf{q}, t) = \left(\varepsilon_q^{1s} - i\gamma_D\right) p_j^{1s}(\mathbf{q}, t) - D_0 E_j(\mathbf{q}, z_0, t) \tag{2}$$

(where γ_D is the dephasing), or, after Fourier transformation,

$$0 = \left(\varepsilon_q^{1s} - i\gamma_D - \hbar\omega\right) p_j^{1s}(\mathbf{q}, \omega) - D_0 E_j(\mathbf{q}, z_0, \omega). \tag{3}$$

We use a massive (parabolic) dispersion $\varepsilon^{1s}_{q_x} = \frac{\hbar^2 q_x^2}{2m_x} + \varepsilon_0^{1s}$ with the exciton mass m_x. Solving the Maxwell equation with a transfer matrix method [60,61] and assuming only outgoing waves (no light field incident on the layer), one obtains the dispersion relation for 2D systems in a form that is by now

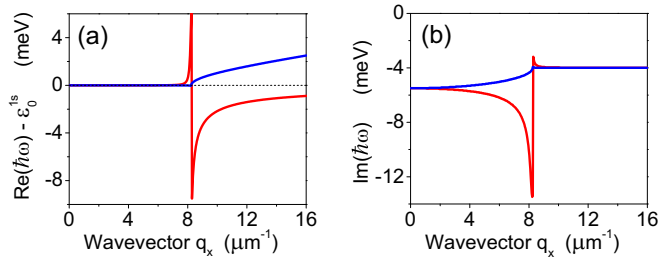

FIG. 2. Real (a) and imaginary (b) part of the dispersion relation of longitudinal (blue) and transverse (red) 2D-layer polaritons. The dephasing is $\gamma_D = 4$ meV. The edge of the radiative cone is approximately at 8.23 μm^{-1}. The real (imaginary) part of $\hbar\omega_L$ is discontinuous (continuous) at the edge of the radiative cone; the real and imaginary part of $\hbar\omega_T$ are discontinuous.

well known (see, for example, [62,63] and references therein), namely

$$\epsilon_b/k_z - i2\pi\chi(\mathbf{q}, \omega) = 0 \tag{4}$$

for the longitudinal waves, and

$$k_z - i2\pi(\omega^2/c^2)\chi(\mathbf{q}, \omega) = 0 \tag{5}$$

for transverse waves, with the 2D susceptibility

$$\chi(\mathbf{q}, \omega) = \frac{\eta_v |D_0|^2}{\varepsilon_q^{1s} - i\gamma_D - \hbar\omega} \tag{6}$$

and $k_z = \sqrt{\epsilon_b(\omega^2/c^2) - q_x^2}$. The dispersion relation of the 2D-layer polaritons is an implicit equation for $\omega_L(q_x)$ and $\omega_T(q_x)$, respectively, and we choose q_x real valued and ω complex valued. The 2D-layer polaritons are the system's eigenmodes, which are damped (imaginary part of ω) since the system is open. They can be excited by incident radiation that has the same q_x and $\mathrm{Re}(\omega(q_x))$. For solutions outside the radiative cone, excitation schemes usually used for surface-plasmon polaritons can be applied, such as grating-coupling or prism coupling (Kretschmann configuration) [64].

Figure 2 shows an example for the longitudinal and transverse waves using parameters typical for monolayer $MoSe_2$, with $\gamma_D = 4$ meV, inside and outside the radiative cone, which is at $k_c(\omega) = \sqrt{\epsilon_b}(\omega/c)$. These results look similar to those shown in Ref. [65], except for the T branch inside the cone (we believe an effective-mass approximation, which is not valid close to the edge of the radiative cone, was used in that reference). Moreover, [65] finds that both L and T modes inside the radiative cone have a curvature (or effective mass) similar to the free exciton mass, m_x. In Ref. [65], the dephasing was zero or negligible. In our results, the total decay of the eigenmode includes the radiative decay and the dephasing, and therefore the curves for the imaginary parts of $\omega(q_x)$ are approximately shifted by γ_D.

We will now show that the inclusion of the dephasing γ_D has important consequences for the dispersion of the longitudinal 2D-layer dispersion $\omega_L(q_x)$, highlighting the effects of non-Hermitian quantum mechanics, which, as mentioned, had been pointed out in [21] for the case of microcavities. We will analyze the behavior of the L mode inside the radiative cone of a 2D system with a massive radiative resonance. We suppress from now on the subscript L.

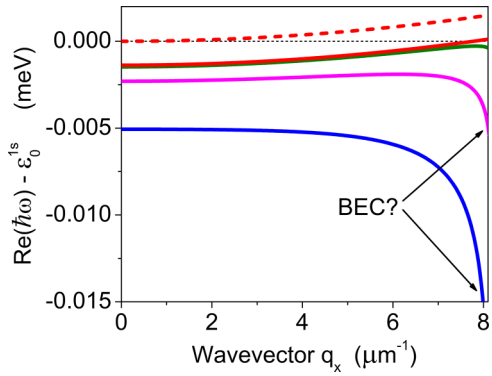

FIG. 3. (a) Same as Fig. 2(a) for longitudinal mode, but only showing inside the radiative cone. (b) Same as (a) for blue curve, plus dispersion for $\gamma_D = 0$ (red curve), 0.1 meV (green), and 1 meV (magenta). The red dashed curve shows the exciton dispersion.

We expand the dispersion relation to lowest order in q_x (which is q_x^2). We write the dispersion $\omega(q_x) = \omega_0 + \Delta\omega(q_x)$ and keep only terms linear in $\Delta\omega(q_x)$. The expression for the real part of $\Delta\omega(q_x)$, being quadratic in q_x, can then be used to define the effective radiative mass m_{Rad} via

$$\mathrm{Re}\hbar\Delta\omega(q_x) = \frac{\hbar^2 q_x^2}{2m_{\mathrm{Rad}}}. \tag{7}$$

The radiative mass depends on the radiative decay rate at $q_x = 0$, $\gamma_R = \frac{2\pi}{\sqrt{\epsilon_b}\hbar c}\eta_v |D_0|^2 \varepsilon_0^{1s}$, and the dephasing γ_D. We find two values of the dephasing, denoted by $\gamma_D^{c(+/-)}$, at which the radiative mass diverges and changes sign. Furthermore, the condition that $\gamma_D^{c(+/-)}$ is real valued is $2\epsilon_b(\varepsilon_0^{1s})^2 \leqslant m_x c^2 \gamma_R[1 + (\gamma_R/\varepsilon_0^{1s})^2]$. Further details are given in the Appendix. We see that a sign change of the radiative mass is only possible if the background dielectric function ϵ_b is sufficiently small. Typical parameter values for freestanding TMD monolayers fulfill the criteria for sign changes, while typical GaAs quantum wells (QWs) with $\epsilon_b \approx 10$ do not. Fabrication techniques (including transfer printing using plastic stamps) of monolayers from van der Waals materials, freestanding or deposited on transparent substrates, have by now become widely available. However, similar techniques have also been developed for thin films or membranes from non-van der Waals materials, for example GaAs microtubes with five monolayer thick [66] and thin (150 nm) GaAs buckled films [67–69] have been fabricated. These techniques could lead to planar GaAs nm-thick membranes with $\epsilon_b \approx 1$, if bending and wrinkling can be avoided [70,71], thus fulfilling the conditions for mass-sign reversal. Alternatively, one could have a dielectric environment with $\epsilon_b \approx 0$, in so-called epsilon-near-zero (ENZ) materials (e.g., [72]). We note, however, that reducing ϵ_b also reduces the radiative cone (Fig. 1), thus limiting the range of wave vectors for in-plane propagation with negative mass.

Continuing the discussion of Fig. 2 for monolayer $MoSe_2$, we see in Fig. 3(a) that for $\gamma_D = 4$ meV the curvature is negative throughout the entire radiative cone, implying a negative radiative mass m_{Rad}. To verify that 4 meV is indeed above the critical value, we show in Fig. 4 the variation of the effective mass as a function of dephasing. We see that

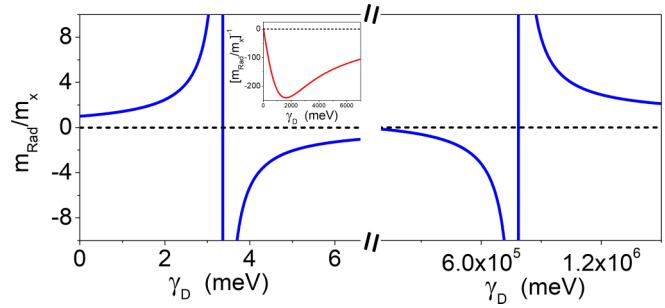

FIG. 4. Radiative mass in units of exciton mass vs dephasing. The inset shows the inverse radiative mass in the region of the extremum.

$\gamma_D^{c(-)} = 3.36$ meV is indeed smaller than 4 meV. As the dephasing goes from zero to infinity, the first singularity of the radiative mass is at $\gamma_D^{c(-)}$. It then has an extremum at about 1.56 eV, and then another singularity at $\gamma_D^{c(+)}$, which for practical purposes does not seem relevant.

If the exciton has a dephasing γ_D smaller than $\gamma_D^{c(-)}$, its in-plane motion is that of a conventional quasiparticle with positive mass. For a dephasing approaching $\gamma_D^{c(-)}$, the exciton behaves like a localized particle as its mass diverges. For a dephasing above $\gamma_D^{c(-)}$, where the effective mass is negative, its kinetic properties are unconventional, with the sign of the velocity being opposite to that of the momentum and particle current. In the limit of large γ_D, where it could approach $\gamma_D^{c(+)}$, the notion of a quasiparticle is no longer applicable, as the lifetime and hence spatial propagation distance goes to zero.

A convenient and simple expression for the radiative mass, analytically obtained in the limit of small wave vectors, is given in the Appendix,

$$m_{\mathrm{Rad}} \approx \frac{m_x}{1 - \gamma_D/\gamma_D^c} \tag{8}$$

[with an approximate form for $\gamma_D^c \equiv \gamma_D^{c(-)}$ given in Eq. (A9)]. This expression clearly shows the divergence and change of sign at $\gamma_D = \gamma_D^c$. It is valid under the conditions given in the Appendix.

It is, however, not only the effective mass, that changes sign as the dephasing increases. Figure 3(b) shows that for (numerically) abitrarily small γ_D, the dispersion relation "rolls over" close to the edge of the radiative cone. This implies that in a higher-order Taylor expansion of $\Delta\omega(q_x)$ we probably have different critical dephasings for each order in q_x^2. Interestingly, the groundstate of the longitudinal 2D-layer polariton is, for many values of γ_D, at the edge of the radiative cone. This brings up the question of possible excitonic Bose-Einstein condensates (BECs) [73]. If the BEC forms at the edge of the radiative cone, then there are two possible scenarios: (i) the BEC emission would be conical (if the entire ring contains the BEC), or there is a second spontaneous symmetry breaking [in addition to the U(1) phase symmetry that is related to the BEC even at zero wave vector] which would choose a certain point on the ring of the radiative cone and thus lead to directed emission with arbitrary direction. However, whether or not a BEC can occur in this system still needs further research, including the issue of opposite temperature requirements (BEC benefits from low temperatures, large dephasing from high

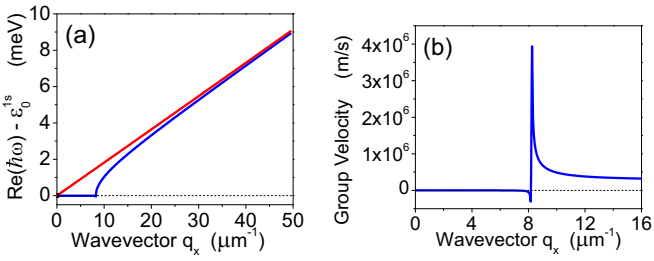

FIG. 5. (a) Blue curve same as blue curve in Fig. 2. The redline shows $\varepsilon^{1s,\mathrm{static}}_{q_x,L}$. (b) Group velocity corresponding to blue curve in (a).

temperatures), and the issue of dispersion. The mathematical form of the dispersion (e.g., massive vs massless [74]) affects the system's ability to undergo BEC transitions. Also, the phase space (3D vs 2D, e.g., [75]) in the vicinity of the energy minimum, which is usually at one point (such as zero wave vector) in wave vector space, affects condensation. In our case the minimum is on a ring in wavevector space. Since, in our case, the kinetics and transport are not described by an effective mass means that the conventional treatment of (cavity) polariton BECs with the Gross-Pitaevskii equation (e.g., [27]) is not applicable, since that equation has a kinetic energy term of a conventional massive particle.

III. INFLUENCE OF ELECTRON-HOLE EXCHANGE INTERACTION

We finally discuss the issue of long-range electron-hole (e-h) exchange interaction, which in TMD monolayers is known to be very strong, and which is related to a linear (in q_x) dispersion (e.g., [22,23,25,30,40,76]). In other words, it has been found to make the exciton massless. This issue has been in principle already addressed in Ref. [65], where it was pointed out that the self-consistent solution of the radiation field and the material response includes the effects of long-range e-h exchange interaction. If the latter is treated with a static Coulomb interaction, then that treatment is only valid at wave vectors much larger than the radiative cone, for example on a wave vector scale that is relevant for the binding of two excitons into a biexciton [76]. However, some publications extend the linear dispersion obtained from a static Coulomb interaction explicitly down to wave vectors inside the cone, where the assumption of static Coulomb interactions and the neglect of radiation retardation effects is not valid [65].

To clarify this point, we show in Fig. 5(a) the dispersion on a wave vector scale six times larger than the radiative cone. We also plot the result from the static calculation (cf. [22–24,31,76]),

$$\varepsilon^{1s,\mathrm{static}}_{q_x,L/T} = \frac{\hbar^2 q_x^2}{2m_x} + \varepsilon_0^{1s} + J^{\mathrm{exch}}_{L/T}(q_x), \tag{9}$$

with $J^{\mathrm{exch}}_{L/T}(q_x) = J^{\mathrm{intra}}(q_x) \pm J^{\mathrm{inter}}(q_x)$. The exchange contributions for L and T are $J^{\mathrm{exch}}_{L}(q_x) = \eta_v 2\pi |D_0|^2 q_x/\epsilon_b$ and $J^{\mathrm{exch}}_{T}(q_x) = 0$, respectively. For L it includes the sum of intervalley and intravalley e-h exchange (these contributions cancel each other for T). Here, we omit q_x-dependent screening, as would be included in the Rytova-Keldysh interaction and improved versions thereof [53]. We see that, at wave vectors considerably larger than the radiative cone (but still small enough for the q_x^2-term to be negligible), the linear dispersion from the e-h exchange is included in $\omega_L(q_x)$, as was noted in Ref. [65]. Importantly, we find that the effect of mass-sign reversal (and more generally dispersion sign reversal) is not affected by the long-range e-h exchange interaction, as it is a phenomenon limited to the inside of the radiative cone. We also show in Fig. 5(b) the group velocity of the L waves, which is relatively large close to the radiative cone, and in our example negative inside the cone.

IV. CONCLUSION

In summary, we have shown that, as a consequence of non-Hermitian coupling, 2D-layer polaritons (without a cavity) can exhibit mass-sign reversal similar to microcavity polaritons and have derived an analytic expression that sets conditions on the mass-sign reversal. We noted that even without the mass-sign reversal, the dispersion can roll over at the radiative cone and discussed hypothetical scenarios for BECs with ground states on a ring. Future research is needed into the condensation behavior in these systems. Our findings may also be relevant for TMD-based lasers (e.g., [77–79]). Finally, we clarified that the long-range e-h exchange interaction does not affect the sign reversal inside the radiative cone.

ACKNOWLEDGMENTS

R.B. acknowledges financial support from the US National Science Foundation (NSF) under Grant No. DMR 1839570, and the use of High Performance Computing (HPC) resources supported by the University of Arizona. J.R.S. acknowledges funding from AFOSR Grant No. FA9550-20-1-0217.

APPENDIX: LIMIT OF SMALL IN-PLANE WAVEVECTORS

In this Appendix, we present additional mathematical details about the 2D-layer polariton dispersion in the limit of small in-plane wave vectors, where the effective-mass approximation is valid.

We expand the dispersion relation given as Eq. (4) in the main text to lowest order in q_x (which is q_x^2). We write the dispersion $\omega(q_x) = \omega_0 + \Delta\omega(q_x)$ and keep only terms linear in $\Delta\omega(q_x)$. For the solution at $q_x = 0$, we find

$$\hbar\omega_0 = \frac{\varepsilon_0^{1s} - i\gamma_D}{1 + i\gamma_R/\varepsilon_0^{1s}}, \tag{A1}$$

where $\gamma_R = \frac{2\pi}{\sqrt{\epsilon_b}\hbar c}\eta_v |D_0|^2 \varepsilon_0^{1s}$ is the radiative decay at $q_x = 0$. This equation contains both the radiative shift of the resonance and its decay. The complex-valued dispersion at nonzero q_x reads (to order q_x^2)

$$\hbar\Delta\omega(q_x) = \frac{1}{1 + i\gamma_R/\varepsilon_0^{1s}}\frac{\hbar^2 q_x^2}{2m_x} + i\frac{\hbar^2 c^2 \gamma_R q_x^2}{2\epsilon_b \varepsilon_0^{1s}\left(\varepsilon_0^{1s} - i\gamma_D\right)}. \tag{A2}$$

For the real part, we therefore obtain

$$\mathrm{Re}\hbar\Delta\omega(q_x) = \frac{1}{1 + \left(\gamma_R/\varepsilon_0^{1s}\right)^2}\frac{\hbar^2 q_x^2}{2m_x} - \frac{\hbar^2 c^2 \gamma_R}{2\epsilon_b \varepsilon_0^{1s}}\frac{\gamma_D}{\left(\varepsilon_0^{1s}\right)^2 + \gamma_D^2} q_x^2. \tag{A3}$$

We can use this equation to define an effective radiative exciton mass m_{Rad} via

$$\mathrm{Re}\hbar\Delta\omega(q_x) = \frac{\hbar^2 q_x^2}{2m_{\mathrm{Rad}}}. \tag{A4}$$

The first term in Eq. (A3) comes from the exciton dispersion and contains a radiative correction to the effective mass. This correction is present even without dephasing. However, in our numerical example, this correction is negligible.

The second term is another radiative correction to the dispersion, but one that is present only if the dephasing is nonzero. Its size depends therefore on the value of γ_D. To get an estimate of the importance of this term, we define a critical dephasing γ_D^c such that the curvature vanishes, $Re\hbar\Delta\omega(q_x;\gamma_D^c) = 0$, or in other words, the radiative 2D-layer polariton mass diverges. We find two critical dephasings,

$$\gamma_D^{c(+/-)} = \frac{1}{2}\varepsilon_{\mathrm{Rad}}\left(1 \pm \sqrt{1 - 4\left(\varepsilon_0^{1s}/\varepsilon_{\mathrm{Rad}}\right)^2}\right), \tag{A5}$$

with $\varepsilon_{\mathrm{Rad}} = \gamma_R[1 + (\gamma_R/\varepsilon_0^{1s})^2]m_x c^2/(\epsilon_b\varepsilon_0^{1s})$. As we will show below, the smaller critical dephasing $\gamma_D^{c(-)}$ is more relevant than $\gamma_D^{c(+)}$, but both give us a complete picture of the evolution of the radiative mass as the dephasing is varied from zero to infinity. The requirement that the square root in this equation is real-valued gives us the following condition for the possibility of a sign reversal of the effective radiative mass:

$$2\epsilon_b\left(\varepsilon_0^{1s}\right)^2 \leqslant m_x c^2\gamma_R\left[1 + \left(\gamma_R/\varepsilon_0^{1s}\right)^2\right], \tag{A6}$$

which can also be written as

$$\epsilon_b^{3/2}\varepsilon_0^{1s} \leqslant \widetilde{m}_x\eta_v|\widetilde{D}_0|^2\widehat{\varepsilon}\left[1 + \left(\gamma_R/\varepsilon_0^{1s}\right)^2\right], \tag{A7}$$

where we define $m_x = \widetilde{m}_x m_0$ (m_0 being the electron mass in vacuum), and $|D_0|^2 = |\widetilde{D}_0|^2 10^{-9}$ eVcm (since in TMDs and GaAs $|D_0|^2$ is approximately 10^{-9} eVcm), and $\widehat{\varepsilon} = \pi m_0 c^2 10^{-9}\,\mathrm{eVcm}/\hbar c \approx 80\,\mathrm{eV}$. The relatively small value of $\widehat{\varepsilon}$ shows that the possibility of the mass-sign reversal depends sensitively on the exact numbers, such as the dielectric constant of the background material and the effective exciton mass. For example, for TMDs we use $|D_0|^2 = 0.96 \times 10^{-9}$ eV cm, $\widetilde{m}_x = 1.67$, $\eta_v = 3$, and $\epsilon_b = 1$ (for free-standing or suspended monolayers, e.g., Ref.s [80–82]), and $\varepsilon_0^{1s} = 1.6\,\mathrm{eV}$. Then the left-hand side (LHS) of Eq. (A7) is 1.6 eV and the right-hand side (RHS) about 384 eV (where we neglect the correction from the square bracket). To estimate a GaAs QW embedded in GaAlAs, we take $|D_0|^2 = 0.46 \times 10^{-9}$ eV cm, $\widetilde{m}_x = 0.2$, $\eta_v = 1$, and $\epsilon_b = 16$. Now the LHS increases to 96 eV (mostly because of the dielectric environment described by the factor $\epsilon_b^{3/2}$), while the RHS reduces to 9 eV. Hence, the condition for mass-sign reversion is not fulfilled. If, however, one could use a free-standing QW membrane (if bending and wrinkling can be avoided), the condition would be fulfilled. Similarly, our numerical values for γ_R, which are 1.5 meV in TMDs and 0.057 meV in GaAs, show that even the large factor $m_x c^2$ is not sufficient for the condition to be fulfilled in GaAs in the presence of a strong dielectric environment. We note that one could have a dielectric environment with $\epsilon_b \approx 0$, in so-called epsilon-near-zero (ENZ) materials. In such an environment, the mass-sign reversal would work even for arbitrarily small m_x and γ_R.

In our numerical example, we find $\gamma_R \ll \varepsilon_0^{1s}$ for TMDs and GaAs, and for TMDs we also find $\gamma_D \ll \varepsilon_0^{1s}$. In the latter case, the expression for the radiative exciton mass simplifies to

$$m_{\mathrm{Rad}} \approx \frac{m_x}{1 - \gamma_D/\gamma_D^c}, \tag{A8}$$

with

$$\gamma_D^c \approx \frac{\hbar^2}{2m_x}\frac{2\epsilon_b\left(\varepsilon_0^{1s}\right)^3}{\hbar^2 c^2\gamma_R}. \tag{A9}$$

Note that this approximate formula, when applied to TMDs, gives a reasonable estimate of $\gamma_D^c = 3.3\,\mathrm{meV}$, while for GaAs this gives a value much larger than ε_0^{1s} and therefore contradicts the assumption for the approximate formula.

We also find that, in the case of infinite exciton mass $m_x = \infty$ (localized excitons), the non-Hermitian coupling creates a finite mass. In this case, the first term in Eq. (A3) is zero, and, to order q_x^2, the second term creates an effective negative mass, for any nonzero dephasing (i.e., $\gamma_D^c = 0$).

[1] Y. Ashida, Z. Gong, and M. Ueda, Adv. Phys. **69**, 249 (2020).
[2] N. Moiseyev, *Non-Hermitian Quantum Mechanics* (Cambridge University Press, Cambridge, 2011).
[3] R. El-Ganainy, M. Khajavikhan, D. N. Christodoulides, and S. K. Ozdemir, Commun. Phys. **2**, 37 (2019).
[4] W. D. Heiss, Phys. Rev. E **61**, 929 (2000).
[5] C. Dembowski, H.-D. Graf, H. L. Harney, A. Heine, W. D. Heiss, H. Rehfeld, and A. Richter, Phys. Rev. Lett. **86**, 787 (2001).
[6] W. D. Heiss, J. Phys. A: Math. Gen. **37**, 2455 (2004).
[7] Y. Choi, S. Kang, S. Lim, W. Kim, J.-R. Kim, J.-H. Lee, and K. An, Phys. Rev. Lett. **104**, 153601 (2010).
[8] M. Liertzer, L. Ge, A. Cerjan, A. D. Stone, H. E. Tureci, and S. Rotter, Phys. Rev. Lett. **108**, 173901 (2012).
[9] T. Gao, E. Estrecho1, K. Y. Bliokh, T. C. H. Liew, M. D. Fraser, S. Brodbeck, M. Kamp, C. Schneider, S. Hoefling, Y. Yamamoto, F. Nori, Y. S. Kivshar, A. G. Truscott, R. G. Dall, and E. A. Ostrovskay, Nature (London) **526**, 554 (2015).
[10] S. Joshi and I. Galbraith, Phys. Rev. A **98**, 042117 (2018).
[11] M. A. Miri and A. Alu, Science **363**, eaar7709 (2019).
[12] L. Pan, S. Chen, and X. Cui, Phys. Rev. A **99**, 011601(R) (2019).
[13] M. Sakhdari, M. Hajizadegan, Q. Zhong, D. N. Christodoulides, R. El-Ganainy, and P. Y. Chen, Phys. Rev. Lett. **123**, 193901 (2019).
[14] K. Kawabata, T. Bessho, and M. Sato, Phys. Rev. Lett. **123**, 066405 (2019).
[15] J. Khurgin, Optica **7**, 1015 (2020).
[16] T. Ohashi, S. Kobayashi, and Y. Kawaguchi, Phys. Rev. A **101**, 013625 (2020).
[17] R. Hanai and P. Littlewood, Phys. Rev. Res. **2**, 033018 (2020).
[18] F. E. Öztürk, T. Lappe, G. Hellmann, J. Schmitt, J. Klaers, F. Vewinger, J. Kroha, and M. Weitz, Science **372**, 88 (2021).

[19] R. Binder and N. H. Kwong, Phys. Rev. B **103**, 085304 (2021).
[20] Y. Li, X. Ma, Z. Hatzopoulos, P. G. Savvidis, S. Schumacher, and T. Gao, ACS Photon. **9**, 2079 (2022).
[21] M. Wurdack, T. Yun, M. Katzer, A. G. Truscott, A. Knorr, M. Selig, E. A. Ostrovskaya, and E. Estrecho, Nat. Commun. **14**, 1026 (2023).
[22] H. Yu, G. Liu, P. Gong, X. Xu, and W. Yao, Nat. Commun. **5**, 3876 (2014).
[23] F. Wu, F. Qu, and A. H. MacDonald, Phys. Rev. B **91**, 075310 (2015).
[24] L. M. Schneider, S. S. Esdaille, D. A. Rhodes, K. Barmak, J. C. Hone, and A. Rahimi-Iman, Opt. Express **27**, 37131 (2019).
[25] M. O. Sauer, C. E. M. Nielsen, L. Merring-Mikkelsen, and T. G. Pedersen, Phys. Rev. B **103**, 205404 (2021).
[26] G. D. Mahan, *Many-Particle Physics* (Plenum Press, New York, 1981).
[27] H. Deng, H. Haug, and Y. Yamamoto, Rev. Mod. Phys. **82**, 1489 (2010).
[28] Here, the adjective "critical" is used to mark a qualitative change in the solution as the parameter (here the dephasing) is varied. Critical dephasing refers to the boundary between positive mass and negative mass solutions. It is not related to concepts in thermodynamics such as critical point, critical exponent, or critical temperature.
[29] M. Bayer, G. Ortner, O. Stern, A. Kuther, A. A. Gorbunov, A. Forchel, P. Hawrylak, S. Fafard, K. Hinzer, T. L. Reinecke, S. N. Walck, J. P. Reithmaier, F. Klopf, and F. Schäfer, Phys. Rev. B **65**, 195315 (2002).
[30] D. Y. Qiu, T. Cao, and S. G. Louie, Phys. Rev. Lett. **115**, 176801 (2015).
[31] A. Steinhoff, M. Florian, A. Singh, K. Tran, M. Kolarczik, S. Helmrich, A. W. Achtstein, U. Woggon, N. Owschimikow, F. Jahnke, and X. Li, Nat. Phys. **14**, 1199 (2018).
[32] T. Deilmann and K. S. Thygesen, 2D Mater. **6**, 035003 (2019).
[33] S. T. Cundiff, H. Wang, and D. G. Steel, Phys. Rev. B **46**, 7248 (1992).
[34] H. Wang, H. Q. Hou, and B. E. Hammons, Phys. Rev. Lett. **81**, 3255 (1998).
[35] C. Sieh, T. Meier, F. Jahnke, A. Knorr, S. W. Koch, P. Brick, M. Hübner, C. Ell, J. Prineas, G. Khitrova, and H. M. Gibbs, Phys. Rev. Lett. **82**, 3112 (1999).
[36] J. P. Prineas, C. Ell, E. S. Lee, G. Khitrova, H. M. Gibbs, and S. W. Koch, Phys. Rev. B **61**, 13863 (2000).
[37] T. Meier, S. W. Koch, M. Phillips, and H. Wang, Phys. Rev. B **62**, 12605 (2000).
[38] C. Phelps, J. Prineas, and H. Wang, Phys. Rev. B **83**, 153302 (2011).
[39] A. M. Jones, H. Yu, N. J. Ghimire, S. Wu, F. Aivazian, J. S. Ross, B. Zhao, J. Yan, D. G. Mandrus, D. Xiao, W. Yao, and X. Xu, Nat. Nanotechnol. **8**, 634 (2013).
[40] D. Y. Qiu, F. H. da Jornada, and S. G. Louie, Phys. Rev. Lett. **111**, 216805 (2013).
[41] X. Liu, T. Galfsky, Zh. Sun, F. Xia, E. Lin, Y. Lee, S. Kena-Cohen, and V. Menon, Nat. Photon. **9**, 30 (2015).
[42] A. Chernikov, T. C. Berkelbach, H. M. Hill, A. Rigosi, Y. Li, O. B. Aslan, D. R. Reichman, M. S. Hybertsen, and T. F. Heinz, Phys. Rev. Lett. **113**, 076802 (2014).
[43] Z. Ye, T. Cao, K O'Brien, H. Zhu, X. Yin, Y. Wang, S. Louie, and X. Zhang, Nature (London) **513**, 214 (2014).
[44] A. Steinhoff, M. Rosner, F. Jahnke, T. O. Wehling, and C. Gies, Nano Lett. **14**, 3743 (2014).
[45] M. Z. Bellus, F. Ceballos, H. Y. Chiu, and H. Zhao, ACS Nano **9**, 6459 (2015).
[46] Y. You, X. Zhang, T. C. Berkelbach, M. S. Hybertsen, D. R. Reichman, and T. F. Heinz, Nat. Phys. **11**, 477 (2015).
[47] G. Moody, C. K. Dass, K. Hao, C. Chen, L. Li, A. Singh, K. Tran, G. Clark, X. Xu, G. Berghäuser, E. Malic, A. Knorr, and X. Li, Nat. Commun. **6**, 8315 (2015).
[48] H. Yu, X. Cui, X. Xu, and W. Yao, Natl. Sci. Rev. **2**, 57 (2015).
[49] K. Hao, G. Moody, F. Wu, C. K. Dass, L. Xu., C. H. Chen, L. Sun, M. Y. Li, L. J. Li, A. H. MacDonald, and X. Li, Nat. Phys. **12**, 677 (2016).
[50] G. Scuri, Y. Zhou, A. A. High, D. S. Wild, C. Shu, K. De Greve, L. A. Jauregui, T. Taniguchi, K. Watanabe, P. Kim, M. D. Lukin, and H. Park, Phys. Rev. Lett. **120**, 037402 (2018).
[51] I. Niehues, R. Schmidt, M. Druppel, P. Marauhn, D. Christiansen, M. Selig, G. Berghauser, D. Wigger, R. Schneider, L. Braasch, R. Koch, A. Castellanos-Gomez, T. Kuhn, A. Knorr, E. Malic, M. Rohlfing, S. M. de Vasconcellos, and R. Bratschitsch, Nano Lett. **18**, 1751 (2018).
[52] A. V. Stier, N. P. Wilson, K. A. Velizhanin, J. Kono, X. Xu, and S. A. Crooker, Phys. Rev. Lett. **120**, 057405 (2018).
[53] D. Van Tuan, M. Yang, and H. Dery, Phys. Rev. B **98**, 125308 (2018).
[54] P. T. Mahon, R. A. Muniz, and J. E. Sipe, Phys. Rev. B **99**, 235140 (2019).
[55] M. Selig, F. Katsch, R. Schmidt, S. M. de Vasconcellos, R. Bratschitsch, E. Malic, and A. Knorr, Phys. Rev. Res. **1**, 022007(R) (2019).
[56] F. Katsch, M. Selig, and A. Knorr, Phys. Rev. Lett. **124**, 257402 (2020).
[57] A. Chaves, J. G. Azadani, H. Alsalman, D. R. da Costa, R. Frisenda, A. J. Chaves, S. H. Song, D. He, Y. D. Kim, J. Zhou, A. Castellanos-Gomez, F. M. Peeters, Zheng Liu, C. L. Hinkle, S.-H. Oh, P. D. Ye, S. J. Koester, Y. H. Lee, Ph. Avouris, X. Wang, and T. Low, npj 2D Mater. Appl. **4**, 29 (2020).
[58] Y. Yu, C. Ding, R. Binder, S. Schumacher, and C.-Z. Ning, ACS Nano **17**, 4230 (2023).
[59] B. Gu, N. H. Kwong, and R. Binder, Phys. Rev. B **87**, 125301 (2013).
[60] J. Sipe, J. Opt. Soc. Am. B **4**, 481 (1987).
[61] G. Khitrova, H. M. Gibbs, F. Jahnke, M. Kira, and S. W. Koch, Rev. Mod. Phys. **71**, 1591 (1999).
[62] I. Epstein, A. J. Chaves, D. A. Rhodes, B. Frank, K. Watanabe, T. Taniguchi, H. Giessen, J. C. Hone, N. M. R. Peres, and F. H. L. Koppens, 2D Mater. **7**, 035031 (2020).
[63] M. Klein, B. H. Badada, R. Binder, A. Alfrey, M. McKie, M. R. Koehler, D. G. Mandrus, T. Taniguchi, K. Watanabe, B. J. LeRoy, and J. R. Schaibley, Nat. Commun. **10**, 3264 (2019).
[64] N. Peyghambarian, S. W. Koch, and A. Mysyrowicz, *Introduction to Semiconductor Optics* (Prentice Hall, New Jersey, 1993).
[65] F. Tassone, F. Bassani, and L. C. Andreani, Nuovo Cimento D **12**, 1673 (1990).
[66] N. Ohtani, K. Kishimoto, K. Kubota, S. Saravanan, Y. Sato, S. Nashima, P. Vaccaro, T. Aida, and M. Hosoda, Physica E **21**, 732 (2004).
[67] Y. Sun, S. Kim, I. Adesida, and J. A. Rogers, Appl. Phys. Lett. **87**, 083501 (2005).

[68] Y. Sun, E. Menard, and J. A. Rogers, Appl. Phys. Lett. **88**, 183509 (2006).
[69] Z. Xue, H. Song, J. A. Rogers, Y. Zhang, and Y. Huang, Adv. Mater. **32**, 1902254 (2020).
[70] Y. Sun, W. M. Choi, H. Jiang, Y. Y. Huang, and J. A. Rogers, Nat. Nanotechnol. **1**, 201 (2006).
[71] P. Cendula, S. Kiravittaya, Y. F. Mei, Ch. Deneke, and O. G. Schmidt, Phys. Rev. B **79**, 085429 (2009).
[72] I. Liberal and N. Engheta, Nat. Photon. **11**, 149 (2017).
[73] Y. Morita, K. Yoshioka, and M. Kuwata-Gonokami, Nat. Commun. **13**, 5388 (2022).
[74] S. Fujita, T. Kimura, and Y. Zheng, Found. Phys. **21**, 1117 (1991).
[75] F. Dalfovo, St. Giorgini, L. P. Pitaevskii, and S. Stringari, Rev. Mod. Phys. **71**, 463 (1999).
[76] N. H. Kwong, J. R. Schaibley, and R. Binder, Phys. Rev. B **104**, 245434 (2021).
[77] Y. Ye, Z. J. Wong, X. Lu, X. Ni, H. Zhu, X. Chen, Y. Wang, and X. Zhang, Nat. Photon. **9**, 733 (2015).
[78] S. Wu, S. Buckley, J. R. Schaibley, L. Fengand, J. Yan, D. G. Mandrus, F. Hatami, W. Yao, J. Vucković, A. Majumbar, and X. Xu, Nature (London) **520**, 69 (2015).
[79] Y. Li, J. Zhang, D. Huang, H. Sun, F. Fan, J. Feng, Z. Wang, and C. Z. Ning, Nat. Nanotechnol. **12**, 987 (2017).
[80] K. F. Mak, C. Lee, J. Hone, J. Shan, and T. Heinz, Phys. Rev. Lett. **105**, 136805 (2010).
[81] A. Castellanos-Gomez, R. Roldan, E. Cappelluti, M. Buscema, F. Guinea, H. S. J. van der Zant, and G. A. Steele, Nano Lett. **13**, 5361 (2013).
[82] Y. Zhou, G. Scuri, J. Sung, R. J. Gelly, D. S. Wild, K. De Greve, A. Y. Joe, T. Taniguchi, K. Watanabe, P. Kim, M. D. Lukin, and H. Park, Phys. Rev. Lett. **124**, 027401 (2020).